Optimization of Sintering Temperature and a Qualitative Structure Analysis of $BaFe_2O_4$ using Qualx Software

Dissertation submitted to the University of Kerala
in partial fulfilment of the requirement
for the award of the Degree of

Bachelor of Science
in
Physics

By,

Amritha Suresh	**23019101020**
Mehana Ajayan	**23019101031**
Devika Raj	**23019101009**

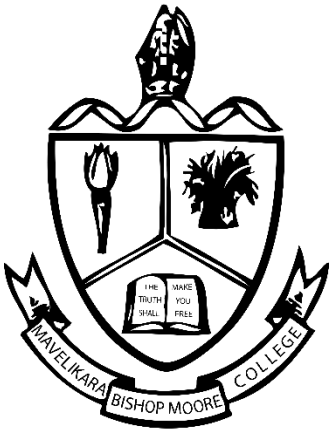

Bishop Moore College, Mavelikara

Alappuzha – 690110

2019-2022

Department of Physics

Bishop Moore College, Mavelikkara

CERTIFICATE

This is to certify that the dissertation entitled **"Optimization of Sintering Temperature and a Qualitative Structure Analysis of $BaFe_2O_4$ using Qualx Software**" by **Amritha Suresh (Reg. No. 23019101020), Mehana Ajayan (Reg. No. 23019101031) and Devika Raj (Reg. No. 23019101009)** for the award of the degree of Bachelor of science in Physics is an authentic work under my supervision and guidance during the period from 2019 – 2022.

Also certified, that the dissertation represents a team work from the part of the candidates.

Dr. Lija K Joy
Assistant Professor
Department of Physics
Bishop Moore College, Mavelikkara

Examiners:

1.

2.

Estd. 1964

DEPARTMENT OF PHYSICS

BISHOP MOORE COLLEGE

Mavelikara, Kerala, India, 690110

Re-assessed and Re-accredited (Third Cycle) with 'A' Grade by NAAC

Supported by DST-FIST, DBT Star College & KSCSTE SARD Schemes

Certificate

*This is to certify that the work presented in this dissertation entitled "**Optimization of Sintering Temperature and a Qualitative Structure Analysis of BaFe2O4 using Qualx Software**" by **Amritha Suresh (Reg. No. 23019101020), Mehana Ajayan (Reg. No. 23019101031) and Devika Raj (Reg. No. 23019101009)** is a record of original research carried out by them under my supervision and guidance in partial fulfillment of the requirements of the Bachelor of Science in Physics. Neither this dissertation nor any part of it has been submitted earlier for any degree or diploma to any institute or university in India or abroad*

Dr. D Sajan
Hod

Dr. Lija K Joy
Supervisor

Kallumala P.O, Mavelikara, Kerala- 690110,Kerala,India, Phone: +91-479 230 3260,Fax: +91-479 230 3260
Website :www.bishopmoorecollege.org, Email: hodbmcphysics@gmail.com

Declaration of Originality

We, **Amritha Suresh (Reg. No. 23019101020), Mehana Ajayan (Reg. No. 23019101031) and Devika Raj (Reg. No. 23019101009)** hereby declare that this dissertation entitled

"Optimization of Sintering Temperature and a Qualitative Structure Analysis of $BaFe_2O_4$ using Qualx Software"

represents our original work carried out as a Bachelor of Science student of University of Kerala and to the best of our knowledge, it contains no material previously published or written by another person, nor any material presented for the award of any other degree or diploma of University of Kerala or any other institution. Any contribution made to this research by others, with whom we have worked at University of Kerala or elsewhere, is explicitly acknowledged in the dissertation. Works of other authors cited in this dissertation have been duly acknowledged under the section "Reference". We are fully aware that in case of any non-compliance detected in future, the Senate of University of Kerala may withdraw the degree awarded to me on the basis of the present dissertation.

Amritha Suresh

Mehana Ajayan

Devika Raj

Acknowledgements

We express our sincere gratitude to everyone who has helped us with this project. And also, we thank the Almighty God for having strengthened us and made us capable of doing all these works.

We wish to convey our deep sense of gratitude to our respected principal **Dr. Jacob Chandy**, for providing us with all our needs and lab facilities even in such a pandemic situation and considering. And we are indebted to our **HOD Lt. Dr D Sajan** for helping us throughout this project and providing us with valuable advice and guidance. We express our heartfelt gratitude to our project guide **Dr Lija K Joy** for providing us whole hearted advice, help and support. We are also very thankful to our warden **Dr Jerin Susan John** and all other teaching and non-teaching staff in our department for supporting us and giving the instructions.

We would also like to extend our sincere gratitude to **Mr. Arun Raj R S** and **Ms Aruna Joseph** for providing us all the help and support throughout the project, especially in the synthesis of the compound.

We use this opportunity to express our thanks to all faculty members in Bishop Moore College, Mavelikara for their kind and constant support and for helping to finish the project. Also thanks to DST-FIST, DBT-STAR, KSC-STE SARD schemes for financial and technical support for our project. We would also thank to researchers in St Thomas College, Pala for the XRD measurement.

Last but not least we thank our parents and friends for their deep support and help which made the completion of this project possible.

Amritha Suresh

Mehana Ajayan

Devika Raj

Abstract

Spinel ferrites with the general formula of AFe_2O_4 (A – divalent cations) are one of the most frequently encountered structure types in inorganic chemistry. Spinel is often used as a data storage device due to its ferromagnetic property at room temperature and is also used as catalysts for reactions at high temperatures due to its high-temperature stability. In spinel ferrites, Alkaline earth metal ferrites have considerable attention due to their potential application as magnetic materials in the various electronic, magnetic and microwave devices. Barium ferrite is often used in the manufacture of pigments, magnetic storage media, permanent magnets and magneto material, as well as in the absorption of electromagnetic waves. This material has a high magnetization at room temperature, high coercivity, high chemical stability, as well as photocatalytic properties against different organic dyes. To get phase pure barium ferrite, different synthesis techniques have been developed, such as microemulsion, hydrothermal reaction, glass crystallization, salt-melt technique etc.

In this work, $BaFe_2O_4$ was synthesized via the glycine glycol assisted sol-gel method. The synthesized powder was characterized by X-ray diffraction. Phase identification of the obtained powder was determined by using Qualx free software. XRD pattern confirms $BaFe_2O_4$ exhibits orthorhombic structure at 1200^0 C sintering temperature

Contents

List of Figures

Chapter-1
General Introduction

Nanotechnology is referred to as the science, engineering and technology conducted at the nanoscale, which has a size of about 1 to 100 nanometers. Nanotechnology is called the technology of the next century as it is a centre of attraction for researchers because of its wide variety of applications in biomedical, optical and electronic fields. The technology promises scientific advancement in many sectors such as medicine, consumer products, energy, materials and manufacturing. A life without nanotechnology is impossible for us as it has made a tremendous influence on human life and society.

1.1 Ferrites

Ferrites are ceramic-like materials having magnetic properties that are useful in several types of electronic devices. They are ferromagnetic oxide materials composed of iron oxide and one or more other metals in a chemical combination. A ferrite is formed by the reaction of ferric oxide (iron oxide or rust) with any of several other metals such as magnesium, barium, aluminium, manganese, copper, nickel, cobalt or iron itself. Ferrites are similar to ceramic materials with magnetic properties that are useful in many types of electronic devices.

They have high permeability along with high resistivity. Their saturation magnetization is less than half of ferromagnetic alloys. They have high heat resistance and corrosion resistance.

Ferrites are ferrimagnetic ceramic compounds. They are brittle, poor, iron-containing and hard conductors of electricity. Ferrites are generally grey or black, made up of a large number of small crystals and are polycrystalline. They are derived from iron oxides and are usually described by the formula $M(Fe_xO_y)$, where M represents any metal that forms divalent bonds, such as any of the elements mentioned earlier. Nickel ferrite ($NiFe_2O_4$)and Manganese ferrite ($MnFe_2O_4$). Ferrites exhibit a kind of magnetism called ferrimagnetism, which is different from the ferrimagnetism of materials like iron, cobalt and nickel. The magnetic moments of constituent atoms in ferrites align themselves in two or three different directions.

Ferrites have importance in engineering and technology because they possess spontaneous magnetic moments below the curie temperature. Ferrite materials have extremely low costs, are made of iron oxide and also have excellent corrosion resistance. Ferrates can be classified based on structure and magnetic properties.

1.2 Classification of Ferrites Based on Structure

Ferrites are classified as follows based on their structure.

i. Spinel Ferrite
ii. Garnet
iii. Orthoferrite
iv. Hexagonal Ferrite

1.2.1.Spinel Ferrite

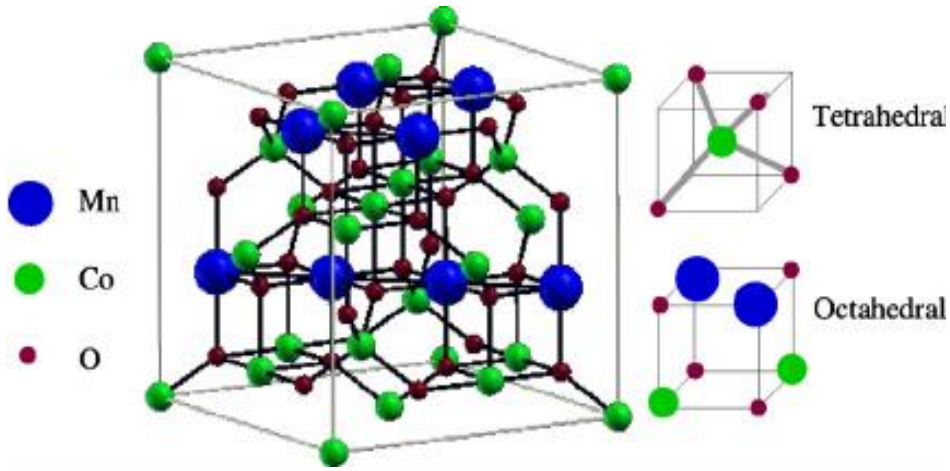

Figure 1.1 Structure of Spinel Ferrite

A spinel ferrite possesses two interstitial sites: a tetrahedral (A) and an octahedral (B). The chemical formula of spinel ferrite is MFe_2O_4, where M stands for divalent metal ions. It is possible to accommodate a variety of cations at the tetrahedral A site and octahedral B site, giving rise to a wide range of properties for ferrites. M can be replaced by other divalent metal ions, and spinel ferrites can be created in any number of configurations. A combination of divalent and tetravalent ions can also be used to replace Fe^{3+} ions. Examples of trivalent ions that can replace Fe^{3+} ions include Al^{3+}, Cr^{3+}, Ga^{3+} etc.

Many applications of these materials have been developed, including magnetic

recording media, antenna rods, loading coils, microwave devices, and core materials for power transformers in electronics and telecommunication.

1.2.2.Garnet

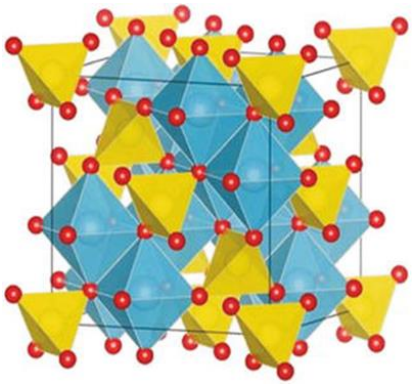

Figure 1.2 Garnet Structure

Garnet type ferrites are described by the formula: $Me_3Fe_5O_{12}$, where Me is a trivalent ion, such as rare earth or yttrium. A unit cell of a garnet type ferrite contains eight molecules (160 atoms). Normally, metal ions are distributed in three types of sites: dodecahedral, tetrahedral and octahedral sites. The Fe^{3+} ions occupy the tetrahedral and octahedral sites in three-to-two proportions, respectively. The magnetic alignment in spinels occurs through superexchange interaction with intervening oxygen ions, and the interaction is supposed to be stronger the shorter the distance between Me and O and the closer the angle between Me and O. The magnetic moments on the tetrahedral and octahedral cations are arranged antiparallel, and the net magnetic moment antiparallel to those on the dodecahedral sites.

1.2.3. Orthoferrite

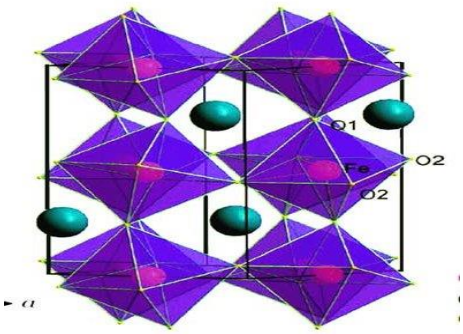

Figure 1.3 Structure of Orthoferrite

Generally, orthoferrites have a formula $MeFeO_3$, where Me represents a large trivalent ion, and Fe represents the iron atom. Orthoferrites are distorted perovskites with an orthorhombic unit cell. Due to the alignment of two antiferromagnetically coupled lattices, these ortho-ferrites show weak ferromagnetism. Despite only being a canting angle of 10-2 radians, this is sufficient to introduce a small net ferromagnetic moment perpendicular to the antiferromagnetic axis. Experimental measurements of Fe spin orientation in $HoFeO_3$ and $ErFeO_3$ at room temperature reveal that the spin axis is parallel to the (100) axis and that it rotates as the temperature drops. At 1.25K, the spin axis is oriented in (001) for $HoFeO_3$ and (110) for $ErFeO_3$.The spin moment on the rare earth ion gets ordered at a much lower Neel temperature.

1.2.4. Hexagonal Ferrite

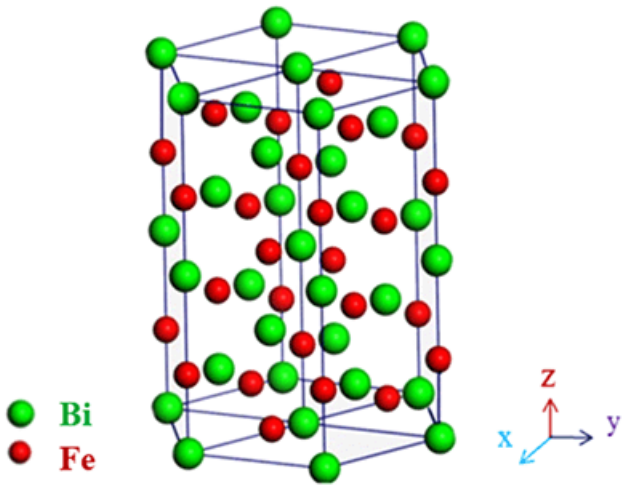

Figure 1.4 Structure of Hexagonal Ferrite

The hexagonal ferrites have gained considerable prominence in recent years due to their hexagonal crystal structure. They are further subcategorized into M, W, Y, Z, and U compounds. Despite their similarities, there are slight differences in their crystal structures, and the M compounds have a simpler structure. Barium ferrite, the well-known hard ferrite, belongs to this class. $MeFe_{12}O_{19}$ is a general formula for these compounds in which Me is a divalent ion of a large ionic radius, such as Ba^{2+}, Sr^{2+}, or Pb^{2+}. It's also possible to have trivalent Me (e.g. La^{3+}, Al, Ga, Cr, Fe). Barium ferrite is a hexagonal crystal structure with two formula units with one iron per unit. A charge compensation is made possible by the presence of Fe^{2+} per formula unit. The oxygen lattice, f.c.c., is similar to the spinel structure in which hexagonal layers of

oxygen are arranged perpendicularly to the (111) direction of the lattice.

1.3 Classification of Ferrites Based on Magnetism

Ferrite can further be classified into two groups based on the magnetism possessed by them.

i. Soft Ferrites

ii. Hard Ferrites

1.3.1. Soft Ferrites

Soft ferrite is a material that is capable of easily reversing the polarity of its magnetization without requiring a considerable amount of the energy necessary to reverse its magnetic polarity. This means that there is only a very small amount of energy lost. Ferrites made from a mixture of iron, nickel, zinc and manganese oxides have a high electrical resistance as well, so they have minimal eddy current losses when they are utilized in inductors and transformers.

1.3.2 Hard Ferrites

Hard ferrites, or permanent magnets, are usually made up of iron or strontium oxides and retain their polarity upon removal of the magnetizing field. Hard ferrite magnets typically consist of barium, iron, or strontium oxides. Their low cost and high coercivity make them a preferred magnet for a variety of applications, including household magnets. They have a wide range of uses.

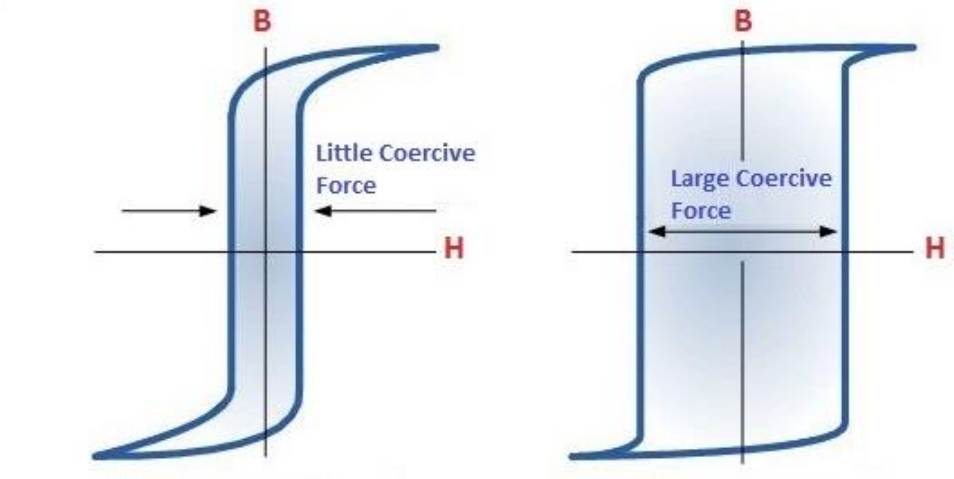

Figure 1.5 Hysteresis curve of soft ferrite and hard ferrite

1.4 Application of Ferrites

Ferrites are widely used owing to their magnetic and crystallographic properties. Below are a few of them.

1. Ferrites have a spontaneous magnetic moment below the curie temperature, just as iron, nickel, cobalt etc does

2. A wide range of applications utilize ferrites, including radar, audio-video, and digital recording and bubble.

3. Microwave coils, frequency devices and computer memory core elements are made with ferrites due to their extremely low eddy current losses

4. Ferrites like ZnO find low-frequency applications in timers. They are also used as switches in refrigerators, air conditioners etc.

5. Ferrite is now used in telephone exchanges, computers, and control equipment.

6. Due to relatively low permeability and flux density compared to iron, ferrites are not suitable for use in the high field and high power applications, such as motors, generators and power transformers, but they can be used in the low field and low power applications.

7. Ferrites are used as ferromagnetic insulators in electrical circuits

1.5. Barium Ferrite

The magnetic materials of normal spinel ferrites with the general chemical formula MFe_2O_4 have various applications owing to a type of M cation, for which M is the divalent metal cation (M^{2+} = Ba^{2+}, Sr^{2+}, Co^{2+}, Mg^{2+}, Zn^{2+}, Cu^{2+}, Mn^{2+}, etc.). The intrinsic properties of $BaFe_2O_4$ nanoparticles, such as high magnetic saturation and coercivity, high chemical and mechanical resistance, and high Curie temperature, have indicated that it is a good candidate for microwave devices, radar-absorbent materials, permanent magnets, drug deliveries, photocatalytic catalysts, credit cards, etc. The methods of synthesizing spinel ferrites greatly affect their properties and applications. In recent decades, extensive research has been performed to improve the synthesis methods to increase crystal purity, decrease the size, and control the morphology of the nanostructures. Diverse methods have been used to prepare

$BaFe_2O_4$ nanoparticles, such as spray pyrolysis, co-precipitation, microemulsion, ball milling, and hydrothermal approaches [1–3]. The crystallinity, size, and shape of the nanostructures are the most influential factors i6 in the properties of nanomaterials.

1.6. Literature Review

There is a wide range of methods developed for the preparation of barium ferrite. Their properties may differ according to their method of preparation. The following literature survey is prepared by referring to some papers.

Reza Peymanfar et.al. prepared $BaFe_2O_4$ nanoparticles by the Sol-Gel Route and investigate their microwave absorption characteristics at Ku-Band frequency using a silicone rubber medium. The $BaFe_2O_4$ nanoparticles were blended with silicone resin and then a hardener was added with 20 wt% to mould a $BaFe_2O_4$/silicone rubber nanocomposite and study the microwave absorption of the nanocomposite. The obtained results demonstrate that $BaFe_2O_4$ nanoparticles were prepared through the sol-gel method using a low sintering temperature and had a significant effect on the crystal purity of the nanostructures. According to the XRD patterns, phase impurities of nanoparticles disappeared when the temperature increased. The FE-SEM micrograph exhibited uniform morphology for $BaFe_2O_4$ nanostructures. The FTIR curve demonstrated that the metal–oxide bonds of $BaFe_2O_4$ nanoparticles had been synthesized at a low temperature. Finally, vector network analysis illustrated that the maximum reflection loss of the $BaFe_2O_4$/silicone rubber nanocomposite was 51.67 dB at 16.1 GHz and that the nanocomposite absorbed more than 94.38% of microwave irradiation along with the Ku-band frequency with a thickness of 1.75 mm. The results suggest that $BaFe_2O_4$ nanoparticles can be a promising microwave absorbing material.

Ravindra Y. Pawar and Satish K. Pardeshi synthesized $BaFe_2O_4$ by citrate gel combustion method. BaFe2O4 spinel-type catalyst is synthesized by a simple and inexpensive one-step citrate gel combustion method, the only method to synthesize soft ferrite other than the Pechini method reported earlier. The precursor and oxide are well characterized by various techniques such as thermogravimetry-differential thermal analysis, Fourier transforms IR, X-ray diffraction, X-ray fluorescence and scanning electron microscopy. The SEM images confirm the coralloid morphology of the $BaFe_2O_4$ catalyst. $BaFe_2O_4$ catalyst shows high activity for styrene oxidation in

the presence of H_2O_2 (30%) as an oxidant in acetone as a solvent. Gas chromatography and mass spectroscopy analysis revealed that conversion of styrene takes place selectively to benzaldehyde up to 88.5 mol% as a major product with a 39.9% yield. The optimization and effect of various reaction conditions on styrene conversion and product distribution were also studied. Ultrasonication exposes active sites on the surface of the catalyst and breaks the hydrophobic cluster to make the reagent available. The better catalytic activity of $BaFe_2O_4$ is due to different site preference energy of individual ions which depend on the ionic size of barium (1.35A°) and iron (0.67A°), the size of interstices and temperature.

In the work by R.A. Candeia et.al, studying the ceramic pigment $BaFe_2O_4$, synthesized by the polymeric precursor method. After calcination at different temperatures, characterizations were done by X-ray diffraction, infrared spectroscopy, surface area by BET, scanning electron microscopy, and UV–vis spectroscopy. The soft chemical synthesis method leads to a high crystallinity material after calcination at 700^0C. The powders were applied to ceramic pieces to evaluate the behaviour of the system when added to a glaze. Pigments presented dark brown colour, with homogeneous surfaces of the glaze. The pigment $BaFe_2O_4$ was obtained by the polymeric precursor method, with a single-phase and brown colour. Diffuse reflectance and chromatic coordinates results indicate that carbonate presence, as well as sintering among particles, change the colour, leading to its variation as a function of the heat treatment of the pigment precursor. Differences between UV–vis spectra of $BaFe_2O_4$ and other ferrites are probably due to the iron ligand field, while the former presents iron in tetrahedral sites, the latter present iron in octahedral and tetrahedral sites. The pigment presents a suitable technological behaviour without reactions between glaze and pigment, indicating that powders are chemically and thermally inert up to 1000^0 C.

Mukesh C. Dimri et. al. synthesized Barium monoferrite ($BaFe_2O_4$) by citrate combustion method. The structural, magnetic properties, as well as permittivity and permeability at microwave frequencies, have been investigated and discussed in the present paper. The formation of orthorhombic crystal structure was confirmed from the X-ray diffraction pattern. These polycrystalline samples sintered at different temperatures have higher Curie temperature (~700 K) and coercivity (~ 4000 Oe) as compared to the values reported in the literature. The high and quite comparable

values of dielectric constant and permeability make this material suitable for use as a microwave absorbing paint as well as a promising electromagnetic interference (EMI) shielding material. An excellent photocatalytic property of $BaFe_2O_4$ was found.

Silvana Da Dalt et.al., synthesized Barium monoferrite $BaFe_2O_4$ which is classified as a permanent magnet stands out among other ceramic magnets due to its high chemical stability, corrosion resistance and low production cost. In addition, experiments conducted on photocatalytic degradation of methyl orange and UV transmittance by spectrophotometry have shown that this material has photocatalytic properties. The spinel ferrite is of importance in many technological areas such as computing, communications and security. Several techniques for synthesis have been studied to optimize the properties of this material. The synthesis of $BaFe_2O_4$ by conventional processes often occurs at temperatures above 1000 °C. In this work, we obtained the phase $BaFe_2O_4$ at low temperatures (600 °C) from the combustion reaction using nitrates and maleic anhydride as metal complexing agents. As for the photocatalytic activity, it was observed that samples annealed at 900 and 1000 °C showed considerable photocatalytic activity, presumably because of the presence of well defined crystalline phases and higher surface areas. The presence of carbon and secondary phases of low crystallinity possibly intervened in the photocatalytic activity of the other samples. Thus, it was possible to combine the highest surface area (9.92 m^2g^{-1}) and the presence of $BaFe_2O_4$ with the best photocatalytic performance.

Abdollah Javidan et.al. synthesized $BaFe_2O_4$ by solid-state thermal decomposition process without using any surfactants or additives. To form pure $BaFe_2O_4$, the as-prepared products were calcined at 800 C for 2 h in a gas mixture of 85 % Ar and 15 % H_2. The saturation magnetization, remanent magnetization, and coercivity of the $BaFe_2O_4$ nanoparticles were 15 emu/g, 5 emu/g, and 2500 Oe, respectively.

R. Dilip and R. Jayaprakash synthesised and characterized $BaFe_2O_4$ nano-ferrites for gas sensor applications. $BaFe_2O_4$ spinel-type ferrite is synthesized by a simple auto-combustion method. The obtained XRD of barium ferrite nanoparticles showed an orthorhombic structure. VSM study shows the high coercivity (Hc) value as 3147.39 Oe and saturation magnetization (Ms) as 33.15 emu/g and confirms it acts as a hard magnetic material. SEM image of the $BaFe_2O_4$ nanoparticles shows spherical-shaped particles with agglomeration. The proposed method is simple, low cost and

compatible with preparing the $BaFe_2O_4$ nanoparticles. The barium ferrite is the most suitable for gas sensors application due to oxidation. This type of ferrites can be used to detect harmful gases and helps to create a clean environment.

Chapter -2

Synthesis Methods and Characterization Techniques

2.1 Synthesis Methods

In terms of morphology, stability, purity, and surface area, the synthesis methods play an important role to produce high-quality ferrites materials. There are many ways through which we can fabricate nanoparticles with desired size, shape, morphology, crystal structure and chemical composition. There are various methods for preparing ferrites but each method have both advantages and disadvantages. Two commonly used methods for the synthesis of nanomaterials are - Bottom-up Approach and Top-down Approach.

2.1.1 Bottom-Up Approach

The bottom-up approach comprises of the assembly of the atoms or molecules into nanostructured arrays due to attractive forces. There are many bottom-up approaches, developed for producing nanoparticles, ranging from the condensation of atomic vapours on surfaces to the coalescence of atoms in liquids. Some of the bottoms-up approach techniques are colloidal precipitation, sol-gel synthesis, hydrothermal synthesis, electrodeposition, flame spray pyrolysis and so on. Even if the technique is cheap, it is difficult to produce on a large scale as well as chemical purification of nanoparticles is also required.

2.1.2 Top-Down Approach

The top-down approach comprises the breaking down of the bulk material into nanosized particles. Top-down approaches are intrinsically simpler and depend either on the removal or division of bulk material to produce the desired structure with suitable properties. The main problem with the top-down approach is the imperfection of surface structure. These techniques involve high-energy wet ball milling, electron beam lithography, atomic force manipulation, gas-phase condensation and so on. Large scale production is possible with this technique.

2.2. Sol-Gel Synthesis

The sol-gel process is a technique for producing solid materials from small molecules. Sol is a colloidal or molecular suspension of particles of ions in a solvent. A gel is a

semi-rigid mass that forms when the solvent from the sol begins to evaporate and the particles or ions left behind begin to join together in a continuous network. This process is a wet-chemical technique that uses either a chemical solution or colloidal particles to produce an integrated network. The precursor for synthesizing these colloids contains usually a metal or metalloid element surrounded by several reactive ligands. The starting material is prepared to form a dispersible oxide and forms a sol in contact with water or dilute acid. In the case of colloid, the volume fraction of particles(or particle density) may be so low that a notable amount of fluid may be required to be removed initially for the gel-like properties to be identified. This can be done in any number of ways. The simplest method is to allow sedimentation to occur initially and then remove the remaining liquid. Phase separation can be accelerated by centrifugation. The remaining liquid(solvent) phase is removed by the drying process, which is generally accompanied by a convincing amount of shrinkage and disinfection. The distribution of porosity in the gel resolves the rate at which the solvent is removed. The ultimate microstructure of the final component will be strongly influenced by changes imposed upon the structural template during this phase of processing. After that, a thermal treatment, or firing process, is often required to accompany further polycondensation and improve mechanical properties and structural stability via final sintering, disinfection and gain growth. The advantage of using this method is that densification is often achieved at a much lower temperature. The sol-gel approach is a cheap and low-temperature technique. Even small quantities of dopants can be introduced in the sol and end up uniformly dispersed in the final product. It can be used in ceramics processing and manufacturing as an investment casting material, or as a means of generating very thin films of metal oxides for different intentions. Sol-gel derived materials are used in optics, electronics, energy, space, biosensors, medicine, reactive material and chromatography. The flow chart of sol-gel synthesis is given below:

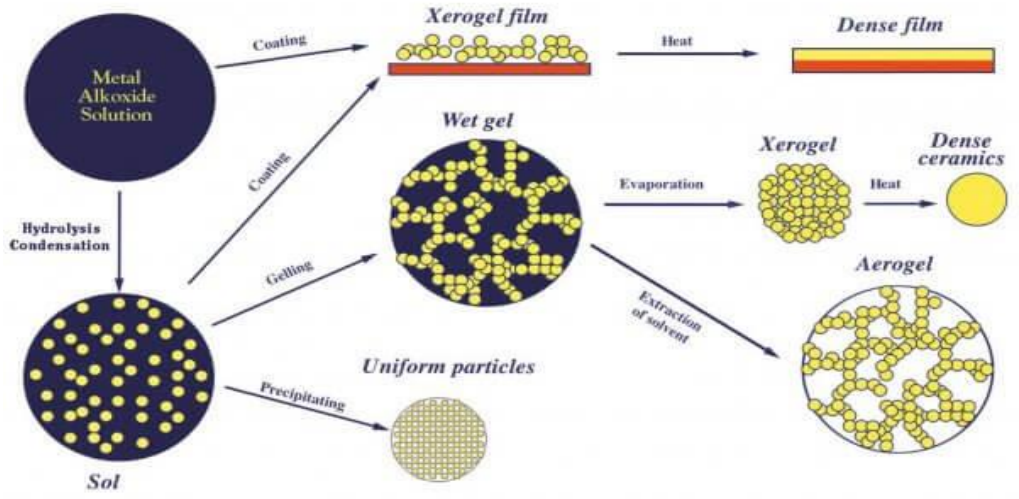

Figure 2.1 Sol-gel Process

2.3 Characterization Techniques

Characterization of nanoparticles is essential to gaining practical knowledge about materials. It can be used to correspond structure with properties. These techniques include scanning electron microscopy, transmission electron microscopy, X-ray diffraction, TEM, XRD, X-ray fluorescence, NMR (nuclear magnetic resonance) and synchrotron techniques. Here, the X-ray diffraction technique is used by us to study the structural information of our compound.

2.3.1 X-ray diffraction technique (XRD)

X-ray diffraction technique (XRD) is a technique used in materials science to analyze the crystallographic structure of a material. It enables verification of the crystallinity and structure of a sample but gives no information of a chemical nature. Fitting XRD patterns can allow calculation of the material lattice parameters, the orientation of a crystal (or grain), the stress in crystalline regions, and secondary phases in the sample. It is generally a bulk characterization technique and produces an average diffraction pattern for the area measured. XRD is a non-destructive technique which can be conducted at room temperature and pressure.

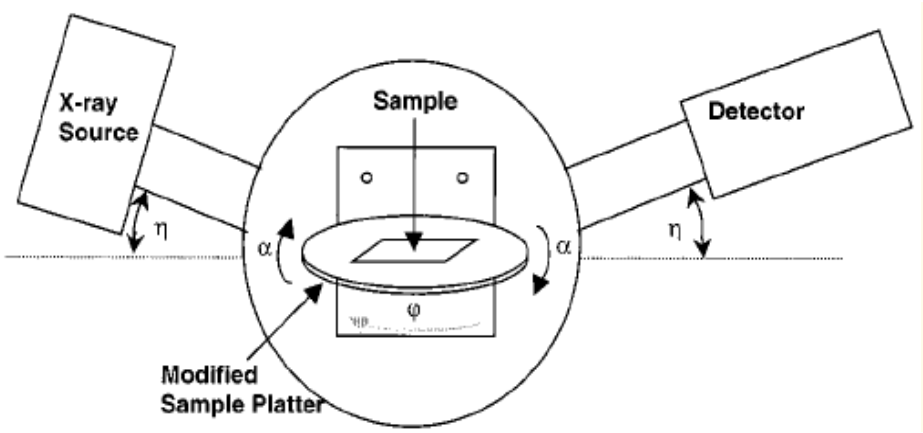

Figure 2.2 Schematic diagram of X-Ray Diffractometer

X-ray diffraction is now a general technique for the study of crystal structures and atomic spacing. X-ray diffraction depends on constructive interference of monochromatic X-rays and a crystalline sample. These X-rays are generated by a cathode ray tube, filtered to create monochromatic radiation, collimated to concentrate, and directed toward the sample. The interaction of the incident rays with the sample produces constructive interference (and a diffracted ray) when conditions satisfy Bragg's Law ($n\lambda=2d \sin\theta$). This law relates the wavelength of electromagnetic radiation to the diffraction angle and the lattice spacing in a crystalline sample. These diffracted X-rays are then detected, processed and counted. By scanning the sample through a range of 2θangles, all possible diffraction directions of the lattice should be attained due to the random orientation of the powdered material. Conversion of the diffraction peaks to d-spacings allows identification of the mineral because each mineral has a set of unique d-spacings. Typically, this is achieved by comparison of d-spacings with standard reference patterns.

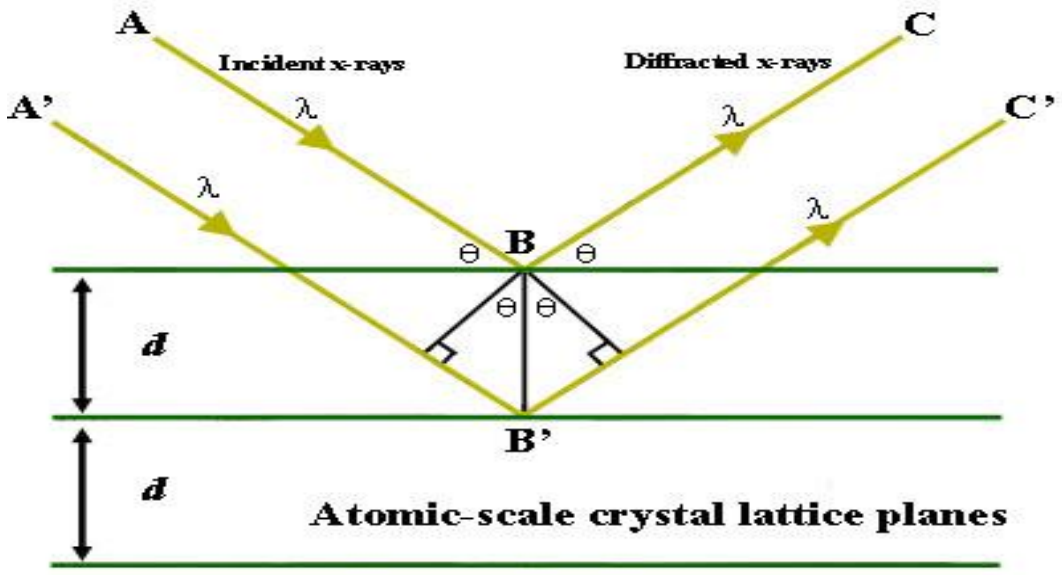

Figure 2.4 Schematic Representation of Bragg's Law

The applications of XRD are as follows:-

- It is the characterization of crystalline materials
- Used to determine unit cell dimensions
- Used to measure the thickness of thin-film and multilayers
- Used in the Pharmaceutical industry
- Used in Forensic studies

Chapter 3

Results and Discussion

3.1 Experimental Procedure for the synthesis of barium ferrite

Barium Ferrite ($BaFe_2O_4$) is prepared by the glycine glycol assisted sol-gel method. In this method, Barium Nitrate $Ba(NO_3)_2$ and iron nitrate $Fe(NO_3)_3$ as the starting materials and citric acid and glycine are used as fuels. The stoichiometric amount of metal salts is calculated and accurately weighted using an electronic weighing balance. Each metal salt was separately dissolved in distilled water and poured into a citric acid solution with a molar ratio of 1:1. Then, an appropriate amount of glycine is added to the solution drop by drop. The resultant solution is stirred for 30 minutes using a magnetic stirrer to obtain a homogeneous solution. Then the solution is placed on a hot plate at around 250 ° C until a dry gel is obtained. After some time, internal combustion occurs in the beaker, yielding a fine brown powder. The resulting powder was thoroughly ground with an agate mortar. The powder is sintered in a furnace for 5 hours at different temperatures (800^0 C, 900^0 C, 1000^0 C and 1200^0 C) to remove impurities and obtain a phase pure $BaFe_2O_4$ powder. After sintering, the powder is thoroughly ground to obtain the fine powder, which is then used to investigate the structural properties of $BaFe_2O_4$ using the XRD technique.

3.2 Phase identification of $BaFe_2O_4$ using Qualx Software

To study the crystal structure and phase purity of $BaFe_2O_4$ samples at different sintering temperatures X-ray diffraction pattern is carried out. The XRD pattern of $BaFe_2O_4$ at different sintering temperatures is shown in figure 3.1. From the figure, it is seen some of the peaks are vanished some have appeared and some have become sharper with increasing sintering temperature. This variation is mainly due to the removal of impure phases and getting high-quality barium ferrite particles with increasing sintering temperature. From the figure, it is seen that at low sintering temperatures, the material exhibits more than two phases simultaneously. When comparing previous reports, it is difficult to identify the phases that occurred in the material. Therefore, to identify the phases that occurred in each sintering temperature of the material and to optimize the sintering temperature to obtain phase pure $BaFe_2O_4$ samples, Qualx software is used.

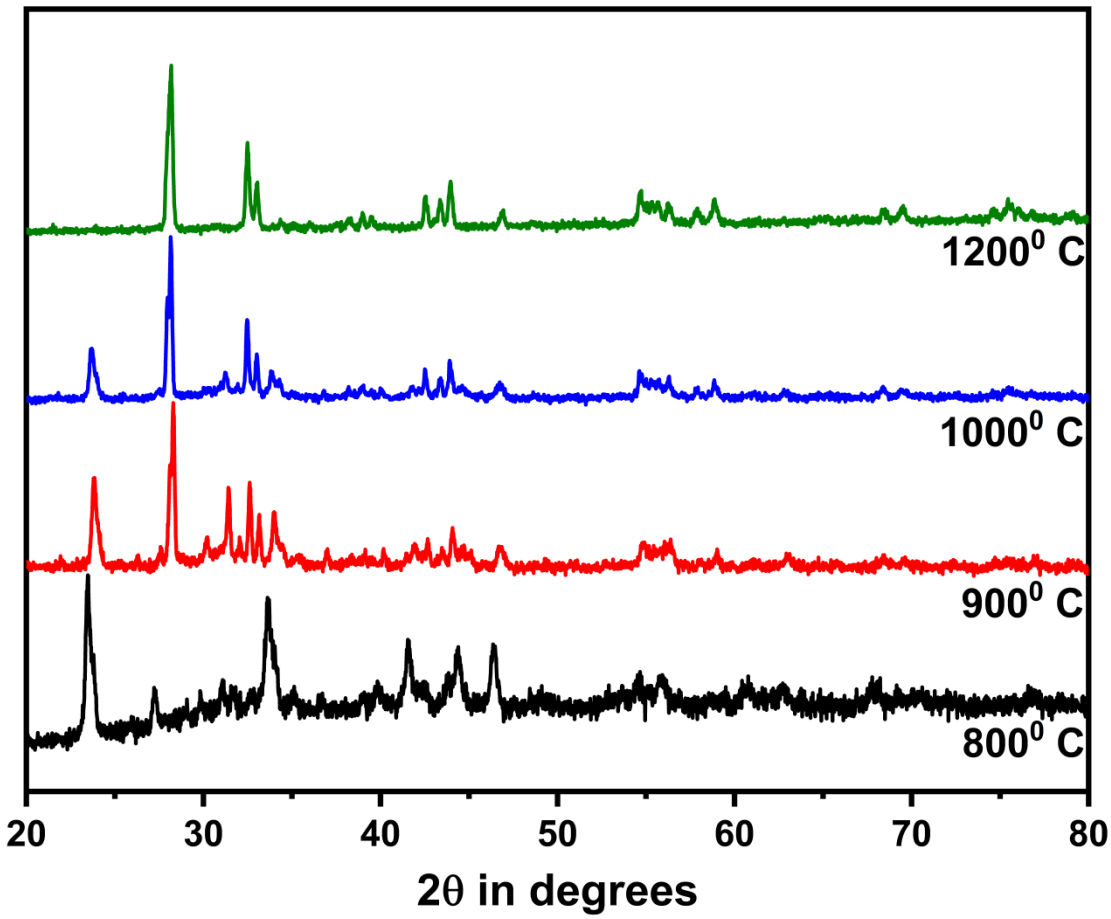

Figure 3.1 XRD pattern of synthesized $BaFe_2O_4$ at different sintering temperature

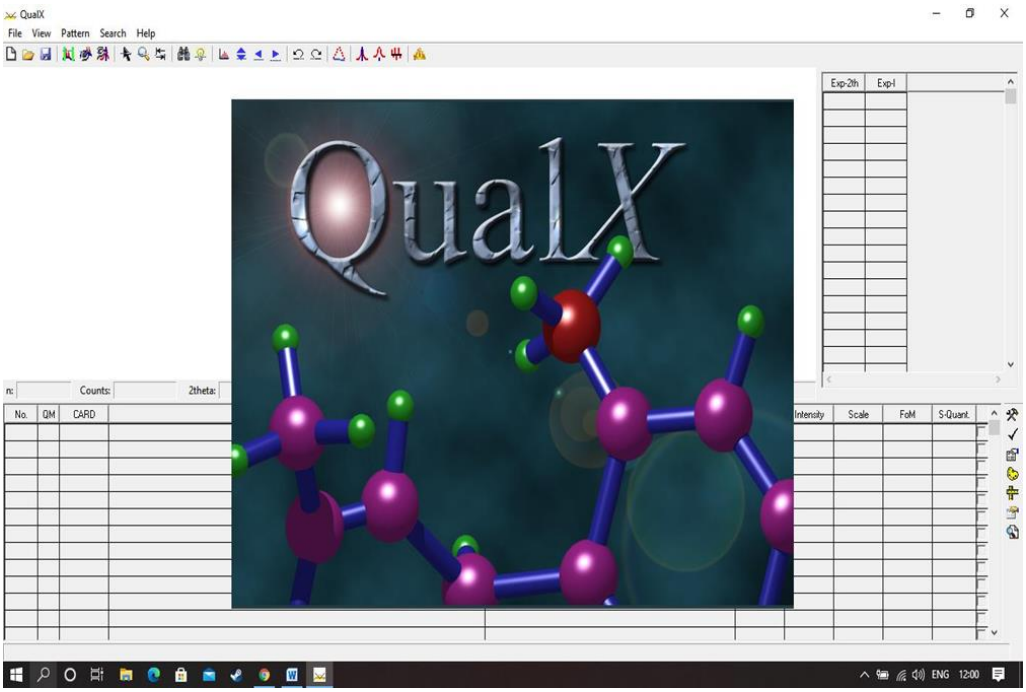

Figure 3.2 Booting Window of Qualx Software

A computer programme called Qualx can identify crystal phases based on powder X-ray diffraction data. It is based on the traditional search–match approach and has a high level of automatism as well as a user-friendly graphic interface. More importantly, this software is completely free and easily accessible to all students, researchers, and teachers. Figure 3.2 represents the Qualx software booting window in the Windows operating system. Following the Qualx booting window, a dialogue box is displayed, as shown in figure 3.3, which is the Qualx software's workspace. It has various menus such as file, pattern, view, search, etc that help us match our results with reported patterns. It has a white background below the menu bar, and our experimental pattern can be plotted in this software in this white space. Two tables can be seen in the right bottom corner of the white space. The peak position and intensity of our XRD pattern can be found on the right side of the window. Following the phase search, the matching phases of our experimental data are listed in the bottom table and will be discussed in detail.

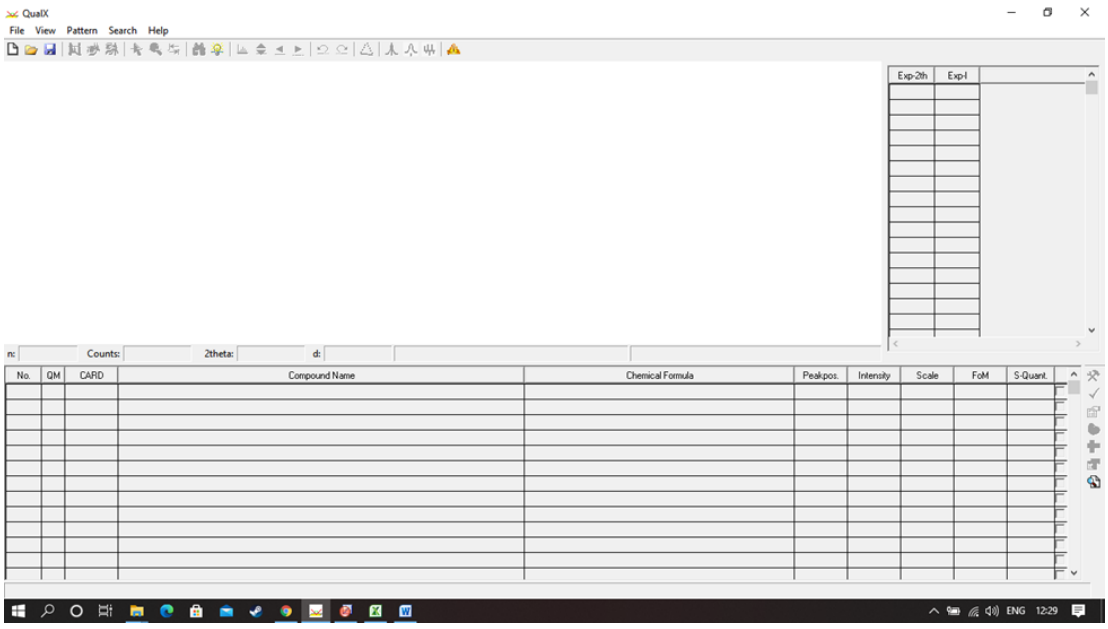

Figure 3.3 Work Space of Qualx Software

The first step in the process of phase identification of our material is importing the experimental diffraction pattern into the Qualx software. Since the Qualx software reads data files more frequently, the files have the extension .dat. Open Qualx software and select the file option, then select the import diffraction data option by double-clicking. This option also has a keyboard shortcut: Ctrl+I. Figure 3.4 shows a dialogue box that appears after selecting the diffraction data file. In this dialogue box, we select the radiation that will be used to generate the XRD diffraction pattern. Cu

radiation is used as the source of X-rays in the present work, so it was chosen for further calculation. Following the selection of the wavelength, we can see a blue-coloured XRD pattern in the white space, as shown in figure 3.5.

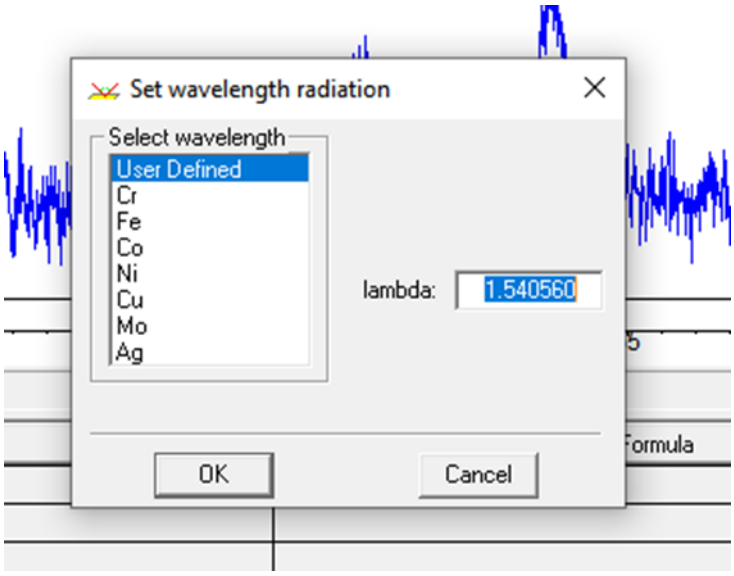

Figure 3.4 Selection Wavelength of Radiation used for taking XRD pattern

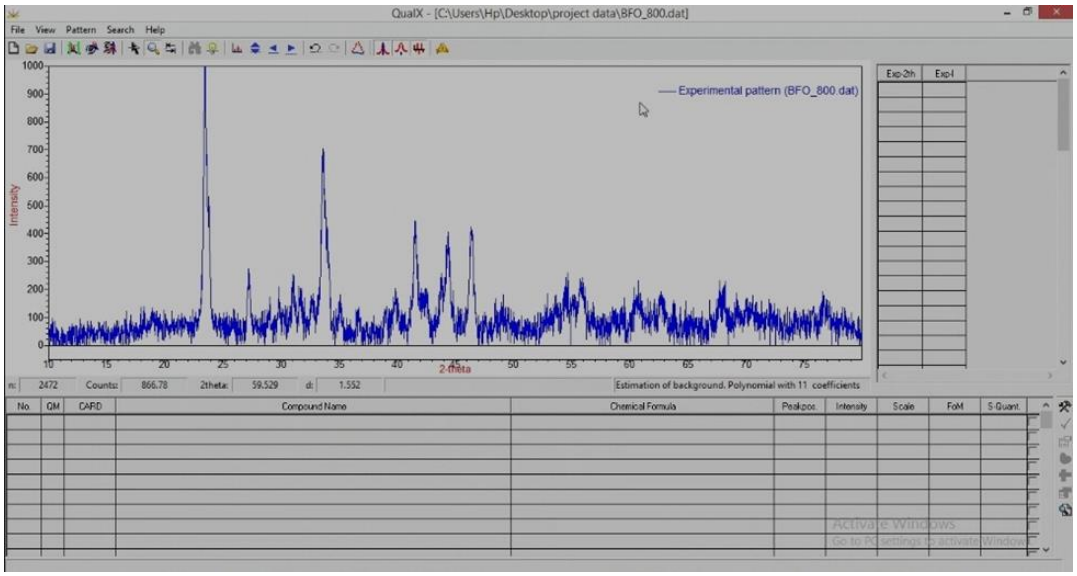

Figure 3.5 Importing experimental patterns into Qualx Software

The next step in our process is to identify the peaks in the pattern. To identify the peaks, go to the pattern menu in the menu bar and double-click the option peak search, as shown in figure 3.6.

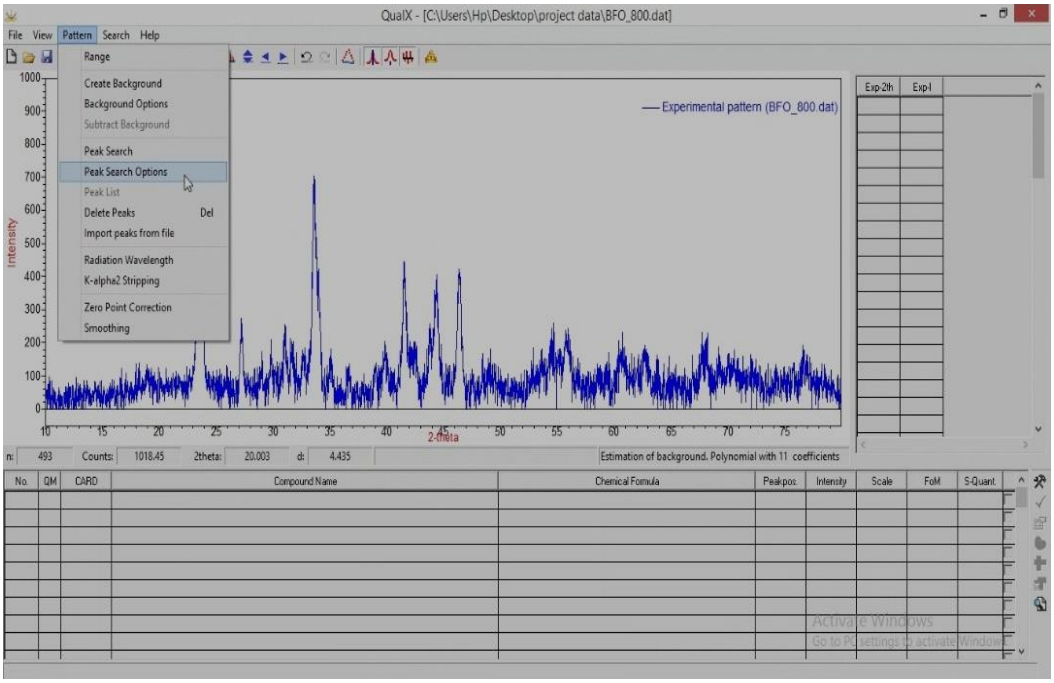

Figure 3.6 Pattern menu

Due to the high sensitivity of the software, more than 300 peaks are observed in the XRD pattern after selecting the peak search, as shown in figure 3.7. To avoid unnecessary peaks, go to the Pattern menu and select the peak Search option, as shown in figure 3.8.

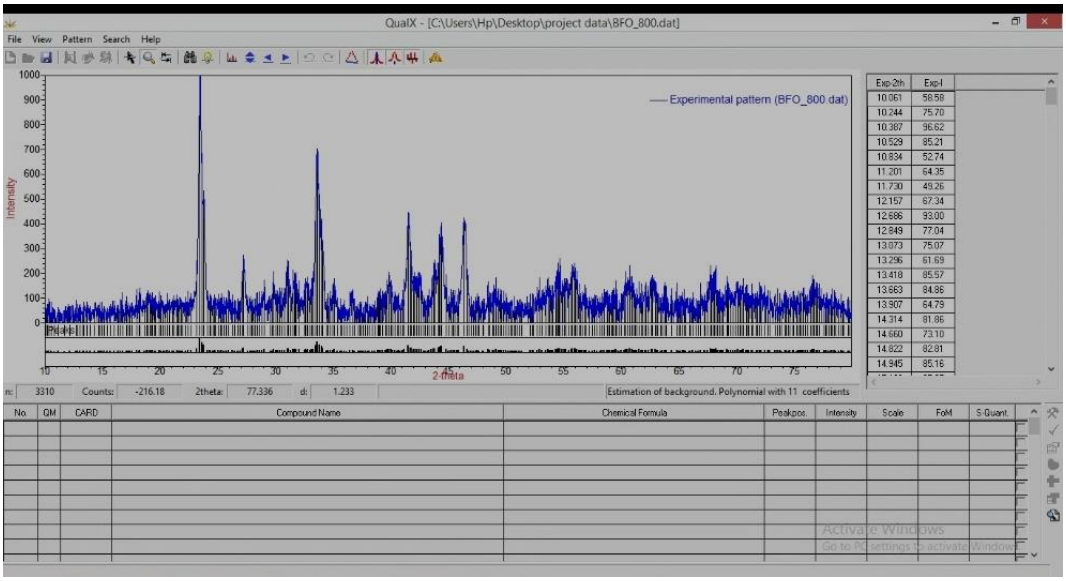

Figure 3.7 Peak searching in Qualx Software

By selecting a peak search option, a new dialogue box appears on the screen named peak search conditions shown in figure 3.9.

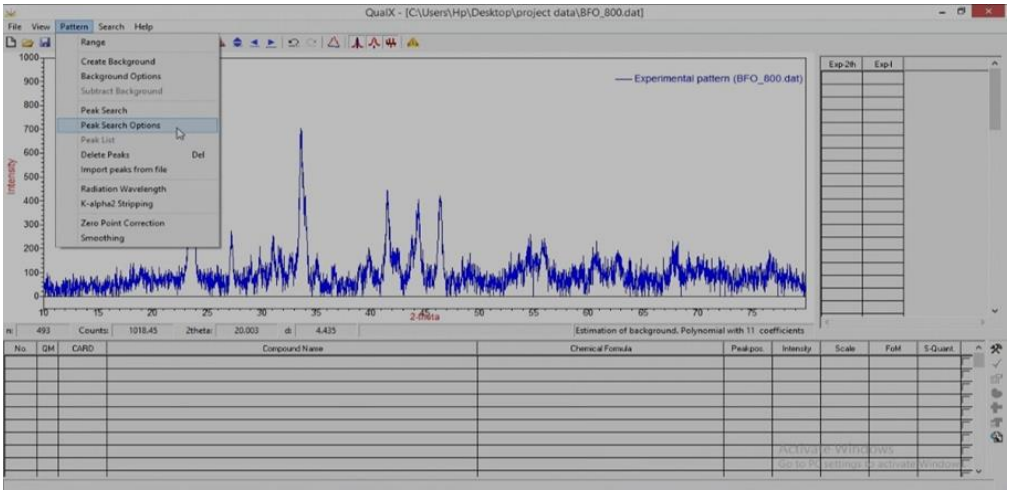

Figure 3.8 Dialog box of Peak Search Conditions

It shows that 346 peaks are found in the XRD pattern, and these unnecessary peaks are removed by adjusting the threshold on intensity and sensitivity and adding/deleting the peak option. Following the application of the appropriate intensity and sensitivity thresholds, the peaks in the XRD pattern are reduced to 46 peaks, as shown in figure 3.10.

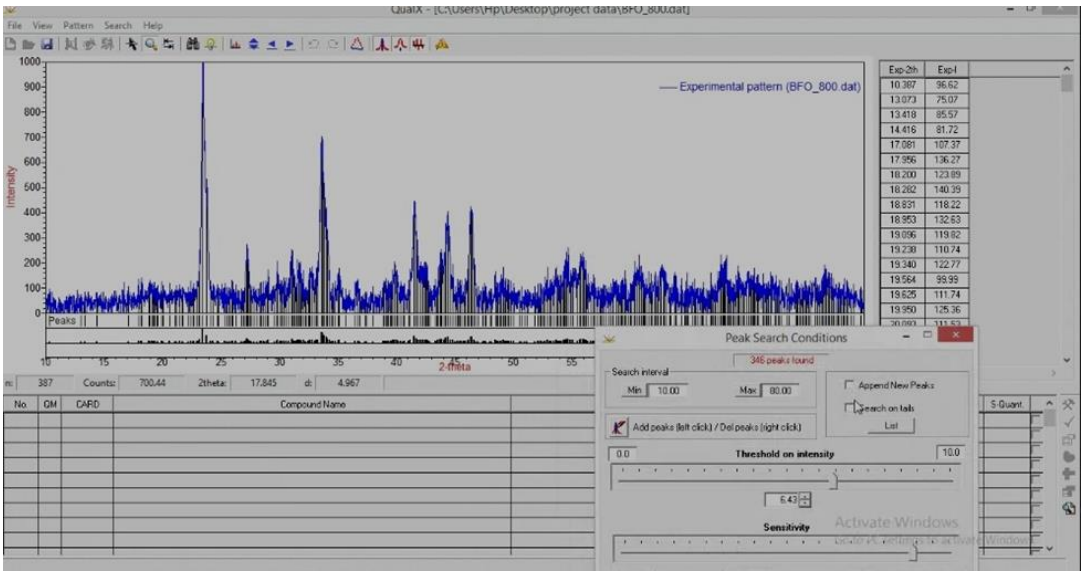

Figure 3.9 Controlling the Number of peaks in the experimental data

After limiting the number of peaks to 46, the pattern is matched to the reported structure in the ICDD or Crystallographic open database. To relate this pattern to reported works, first select the search menu from the menu bar and then click the restraints option, as shown in figure 3.10.

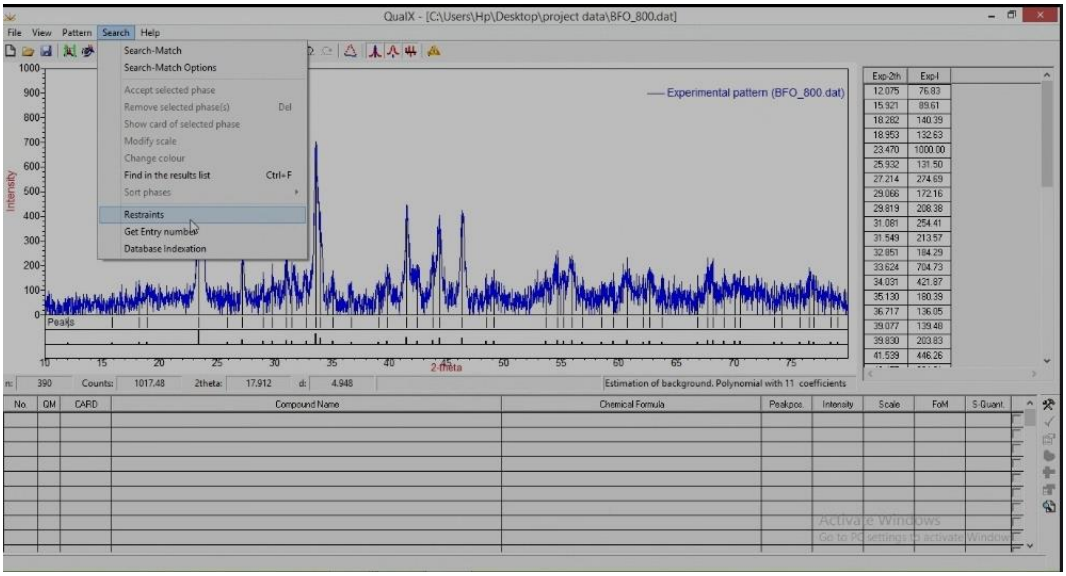

Figure 3.10 Search menu option list

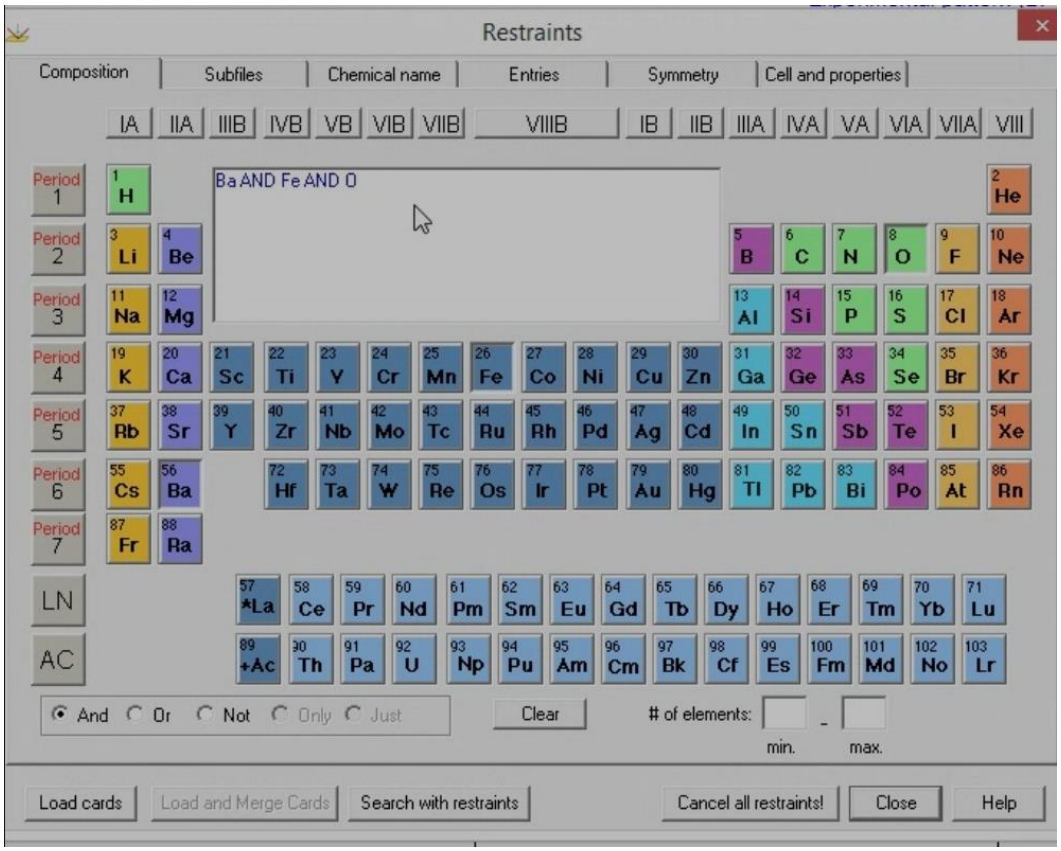

Figure 3.11 Restraint dialogue box in Qualx software

After selecting the restraint menu, a dialogue box displaying the periodic table appears on the screen, as shown in figure 3.11. In that dialogue box, we select the elements that are used in the synthesis, in this case, the elements Fe, O, and Ba. Select the option search with constraints, and the software will search for matching options.

And after the software's search, some compound names will be available in the bottom table, arranged in the order of figure of merit, as shown in figure 3.12. The figure of merit indicates how closely the reported value corresponded to the experimental data. It was found that when the powder was sintered at 800^0 C, three phases occurred simultaneously, and no $BaFe_2O_4$ phase occurred at this sintering temperature.

3.2 Qualitative phase analysis of $BaFe_2O_4$ at different sintering Temperature

(a) Sintering temperature at 800^0 C

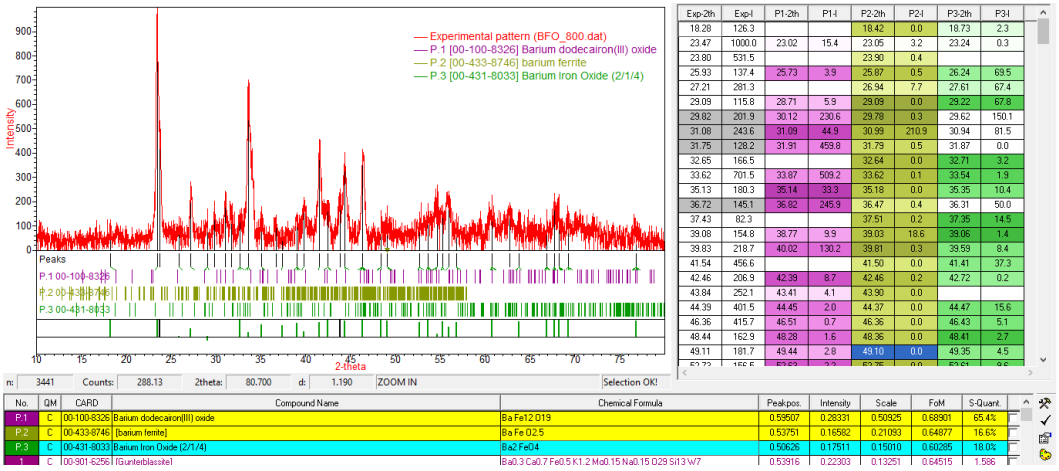

Figure 3.12 Peak Identification of sintered powders at 800^0 C using Qualx Software

The results obtained from qualx software at a sintering temperature of 800^o C are shown in figure 3.12. It is found that at 800^o C, three phases of $BaFe_{12}O_{19}$, $BaFeO_{2.5}$ and Ba_2FeO_4 occurred at a composition of 65.4%, 16.6% and 18% respectively. $BaFe_{12}O_{19}$ exhibit a hexagonal structure with space group *$P6_3/mmc$*. $BaFeO_{2.5}$ exhibit a monoclinic structure with space group *$P12_1/c1$*. Ba_2FeO_4 exhibit a monoclinic structure with space group *$P12_1/n1$*. The crystallographic open database card corresponding to each compound and structure is shown in figure 3.13. It is seen that at 800^0C there is no evidence of $BaFe_2O_4$ phase. To obtain phase pure $BaFe_2O_4$, the ground powder was sintered again at higher temperatures to determine the optimum sintering temperature for $BaFe_2O_4$.

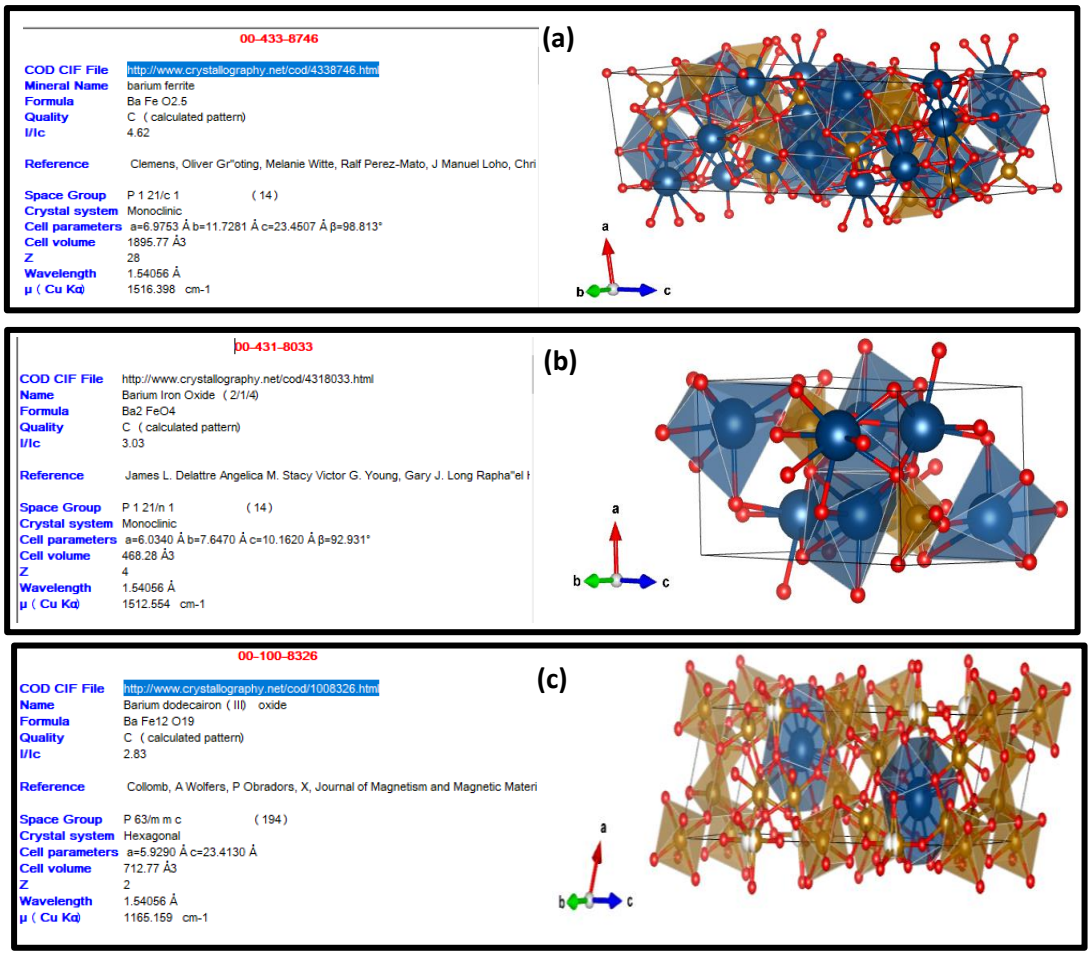

Figure 3.13 COD database card and crystal structure of (a) $BaFeO_{2.5}$ (b) Ba_2FeO_4 (c) $BaFe_{12}O_{19}$

(b) Sintering temperature at 900^0 C

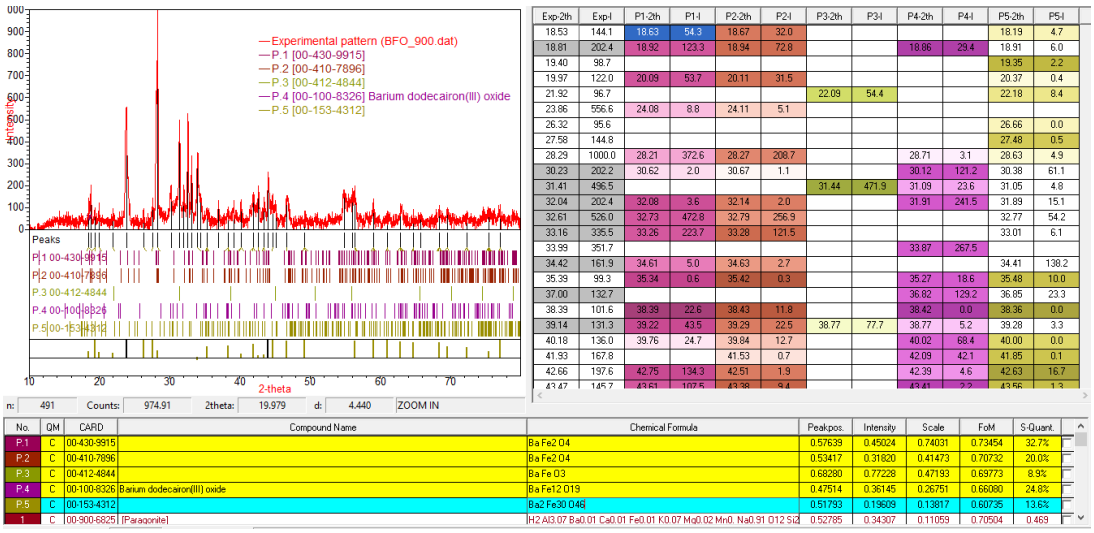

Figure 3.14 Peak Identification of sintered powders at 900^0 C using Qualx Software

The results obtained from qualx software at a sintering temperature of 900^0C are shown in figure 3.14. It is found that 52.7% of $BaFe_2O_4$ phases become appeared. This $BaFe_2O_4$ was again distinguished in two phases with different space groups. Both $BaFe_2O_4$ exhibit an orthorhombic structure with space group $Cmc2_1$ and $Bb2_1m$. The composition of $BaFe_2O_4$ for space group $Cmc2_1$ and $Bb2_1m$ phases are 32.7% and 20% respectively. Besides these phases, three impurity phases are also noticed in the XRD pattern with the help of Qualx Software. They are $BaFeO_3$, $BaFe_{12}O_{19}$ and $Ba_2Fe_{30}O_{46}$ with a composition of 8.9%, 24.8% and 13.6% respectively. These results indicate that the increasing sintering temperature decreases the $BaFe_{12}O_{19}$ phases and it converts them into $BaFe_2O_4$ phases. The crystallographic open database card and structure of each phases are shown in the figure 3.13

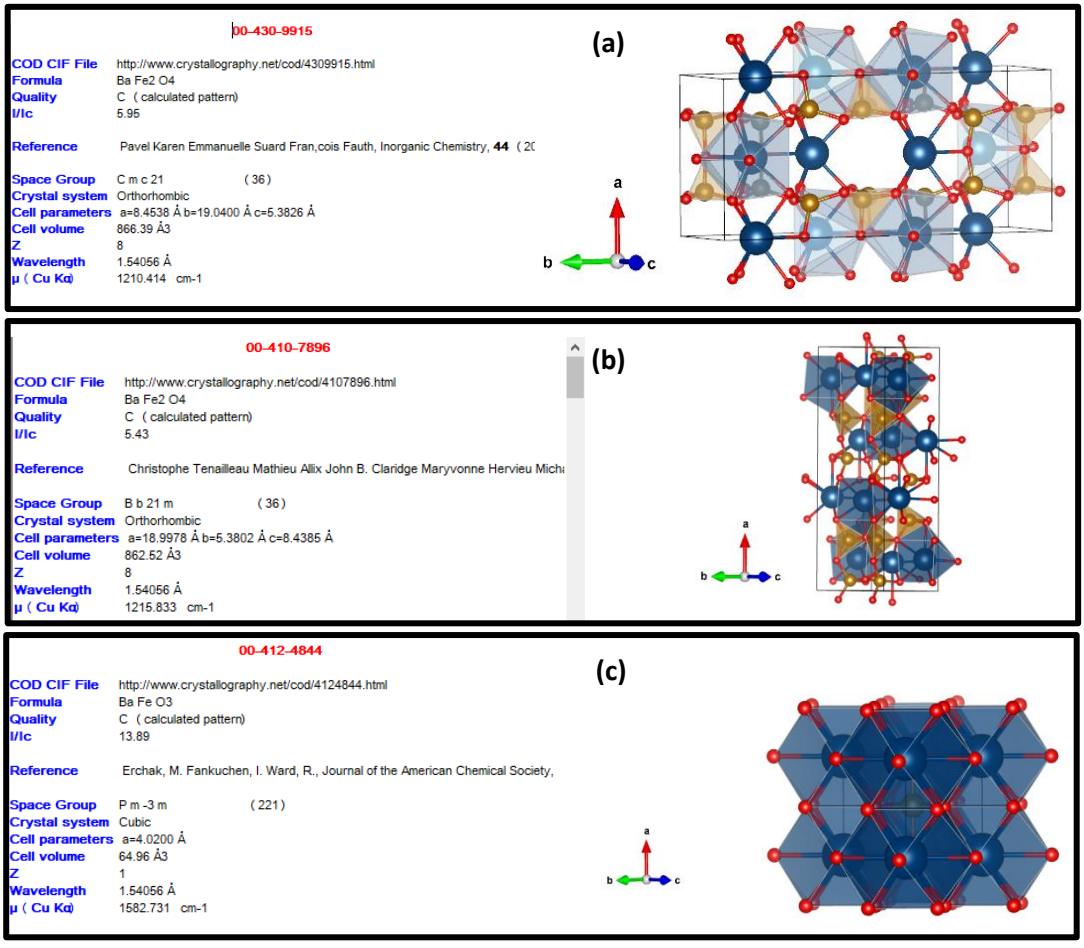

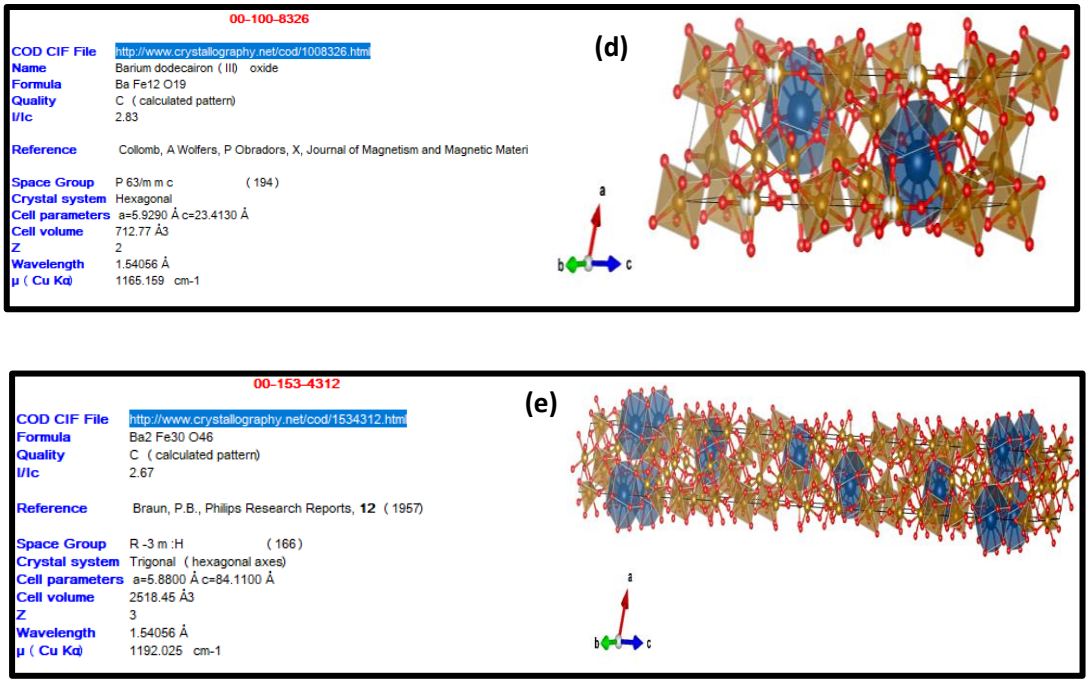

Figure 3.15 COD database card and crystal structure of (a) $BaFe_2O_4$ with space group *Cmc2₁*, (b) $BaFe_2O_4$ with space group *Bb2₁m* (c) $BaFeO_3$ (d) $BaFe_{12}O_{19}$ and (e) $Ba_2Fe_{30}O_{46}$

(c) Sintering temperature at 1000^0 C

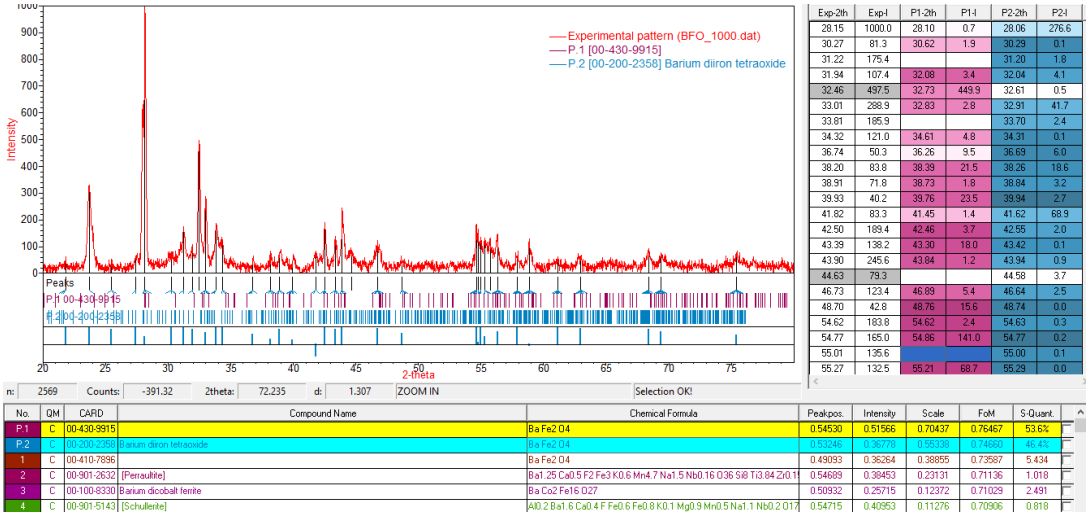

Figure 3.16 Peak Identification of sintered powders at 1000^0 C using Qualx Software

The results obtained from qualx software at a sintering temperature of 1000^0 C are shown in figure 3.16. From this pattern, it is found that at 1000^0 C sintering temperature all impurity peaks are eliminated. Still, $BaFe_2O_4$ shows two phases with different space groups. Both $BaFe_2O_4$ exhibit an orthorhombic structure with space group *Cmc2₁* and *Pmcn*. It can be seen that as the sintering temperature rises from 900

to 1000^0 C, the *Bb2₁m* $BaFe_2O_4$ phase transforms into the most stable $BaFe_2O_4$ phase having space group *Pmcn*. The composition of *Cmc2₁* and *Pmcn* phases are 53.6% and 46.4% respectively. The crystallographic open database card and structure of each phase are shown in the figure 3.17

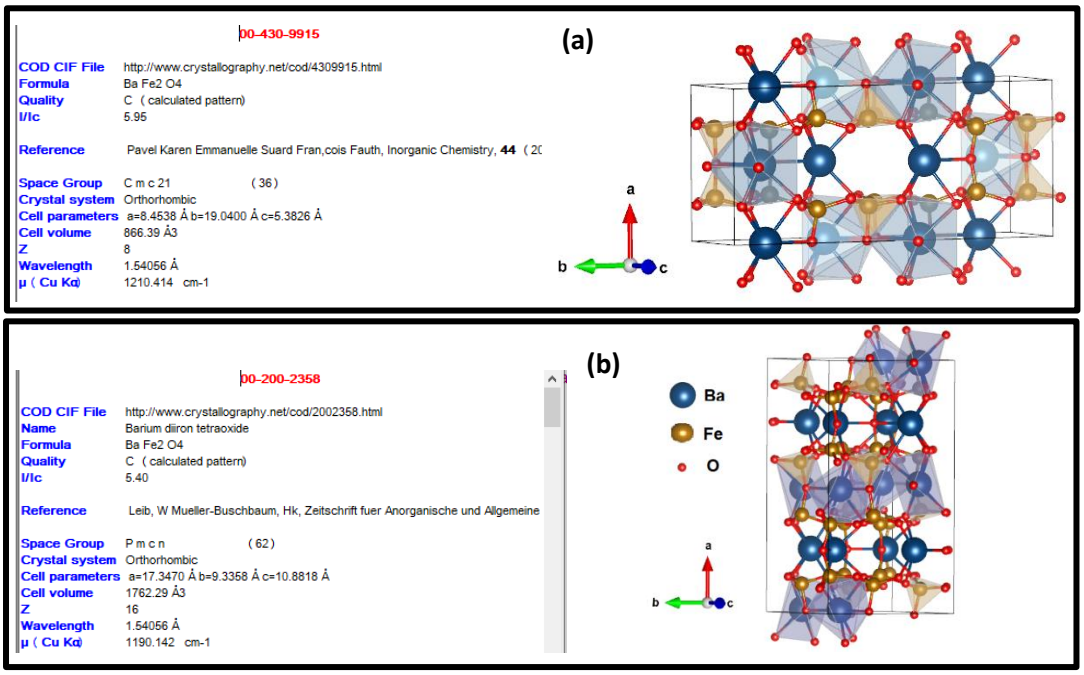

Figure 3.17 COD database card and crystal structure of $BaFe_2O_4$ with space group (a) *Cmc2₁* (b) *Pmcn*

(d) Sintering temperature at 1200^0 C

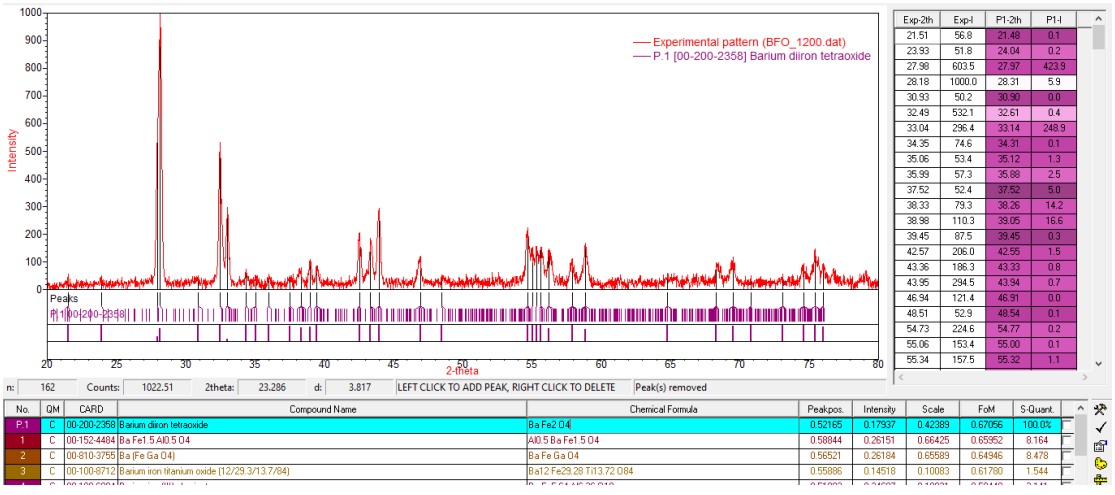

Figure 3.18 Peak Identification of sintered powders at 1200^0 C using Qualx Software

The results obtained from qualx software at a sintering temperature of 1200^o C are shown in figure 3.18. At 1200^o C the XRD pattern shows only one phase of $BaFe_2O_4$ having space group *Pmcn*. This result indicates that to obtain phase pure $BaFe_2O_4$ the

powder sample must be sintered at 1200^{o} C. The most stable state of $BaFe_2O_4$ is the structure exhibiting space group *Pmcn*. The crystallographic open database card and structure of each phase are shown in figure 3.19. From the database card, we can conclude that $BaFe_2O_4$ exhibit an orthorhombic crystal structure with the space group *Pmcn* at sintering temperature 1200^{0} C. The lattice parameters are reported to be a=17.3470 Å, b=9.3368 Å and c=10.8818 Å.

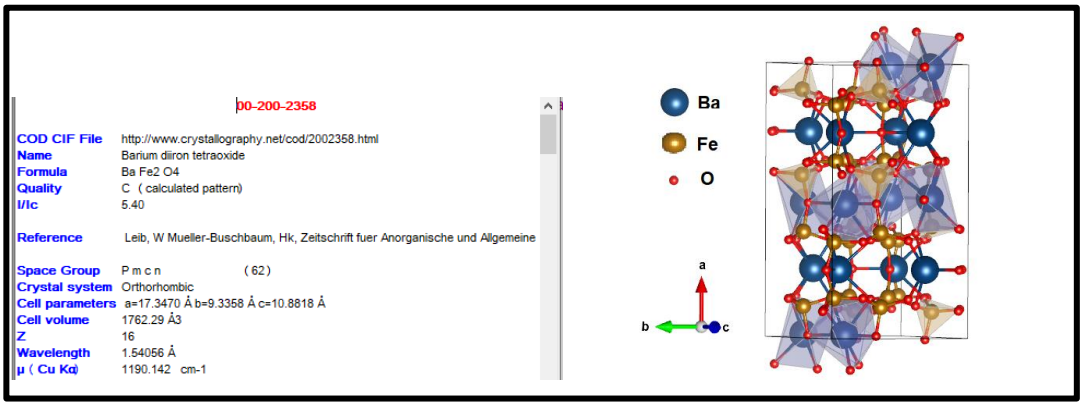

Figure 3.19 COD database card and crystal structure of $BaFe_2O_4$ with space group *Pmcn*

Chapter: 4

Conclusions

Barium ferrite ($BaFe_2O_4$) was successfully prepared by the glycine glycol assisted sol-gel synthesis method. The Qualx software is used to perform qualitative phase identification of the obtained powder at various sintering temperatures. Qualx software is free and has an easy-to-use graphical interface. While phase identification occurred at various sintering temperatures, single-phase $BaFe_2O_4$ occurred at 1200^o C. The resulting $BaFe_2O_4$ had an orthorhombic structure with the space group *Pmcn*. The orthorhombic structure of $BaFe_2O_4$, where the metal ions Fe and Ba are located in tetrahedral and dodecahedral sites, was visualised using the VESTA software. The study on the variation in sintering temperature resulted in the conclusion that $BaFe_2O_4$ is not stable below 1000^o C where exhibits many impurity phases. The increasing temperature eliminated the impurity phases, resulting in a pure $BaFe_2O_4$ phase. As per the qualitative analysis, $BaFe_2O_4$ can have an orthorhombic structure with three different space groups: $Cmc2_1$, $Bb2_1m$, and *Pmcn*. The *Pmcn* space group is the most stable of these and it is obtained ~~in~~ at the high sintering temperature region.

References

[1] Gore Shyam K and Santosh S Jadhav. "Basics of ferrites" Spinel Ferrite Nanostructures for Energy Storage Devices (2020): 1.

[2] Shaikh Shoyeb mohamad F, Mohd Ubaidullah, Rajaram S Mane and Abdullah M. Al-Enizi. "Types, Synthesis methods and applications of ferrites." Spinel Ferrite Nanostructures for Energy Storage Devices (2020): 51.

[3] Jadhav Vijaykumar V., Shubhangi D. Shirsat, Umakant B Tumberphale, and Rajaram S Mane. "Properties of ferrites." In Spinel Ferrite Nanostructures for Energy Storage Devices (2020) 35-50.

[4] Ghule Balaji Gautam, Zeenat Parveen Shaikh, and Rajaram S. Mane. "Ferrites for Batteries." Spinel Ferrite Nanostructures for Energy Storage Devices (2020): 147.

[5] Reza Peymanfar and Mitra Rahmanisaghieh. "*Preparation of neat and capped $BaFe_2O_4$ nanoparticles and investigation of morphology, magnetic, and polarization effects on its microwave and optical performance*" Materials Research Express. **5** (2018) 105012.

[6] Peymanfar, Reza, Mitra Rahmanisaghieh, Arezoo Ghaffari, and Yousef Yassi. "*Preparation and Identification of $BaFe_2O_4$ Nanoparticles by the Sol–Gel Route and Investigation of Its Microwave Absorption Characteristics at Ku-Band Frequency Using Silicone Rubber Medium*." Multidisciplinary Digital Publishing Institute Proceedings **2** (2018): 5234.

[7] Ravindra Y.Pawar, Satish K.Pardeshi. "*Selective oxidation of styrene to benzaldehyde using soft $BaFe_2O_4$ synthesized by citrate gel combustion method*." Arabian journal of chemistry **11** (2018): 282-290.

[8] R.A.Candeia, M.A.F.Souza, M.I.B.Bernardi, S.C.Maestrelli, I.M.G.Santos, A.G.Souza and E.Longo. "*Monoferrite $BaFe_2O_4$ applied as ceramic pigment*." Ceramics International **33** (2007): 521-525.

[9] Mukesh C.Dimri, H.Khanduri, P.Agarwal, J.Pahapill, R.Sternd. "*Structural, magnetic, microwave permittivity and permeability studies of barium*

monoferrite ($BaFe_2O_4$)." Journal of Magnetism and Magnetic Materials **486** (2019): 165278.

[10] Yang Yang, Yinshan Jiang ,Yingwei Wang, Yanbin Sun, Lihua Liu, Jun Zhang. "*Influences of sintering atmosphere on the formation and photocatalytic property of $BaFe_2O_4$.*" Materials Chemistry and Physics **105** (2007): 154-156.

[11] Samira Mandizadeh, Masoud Salavati-Niasari, MinooSadri. ""*Hydrothermal synthesis, characterization and magnetic properties of $BaFe_2O_4$ nanostructure as a photocatalytic oxidative desulfurization of dibenzothiophene."* Separation and Purification Technology **175** (2017): 399-405.

[12] Silvana Da Dalt, Bruna Berti Sousa, Annelise Kopp Alves, Carlos Pérez Bergmann. "*Structural and photocatalytic characterization of $BaFe_2O_4$ obtained at low temperatures*." Materials Research **14** (2011): 505-507.

[13] Abdollah Javidan, Majid Ramezani, Ali Sobhani-Nasab and S. Mostafa Hosseinpour-Mashkani. "*Synthesis, characterization, and magnetic property of monoferrite $BaFe_2O_4$ nanoparticles with aid of a novel precursor*." Journal of Materials Science: Materials in Electronics **26** (2015): 3813-3818.

[14] R. Dilip and R. Jayaprakash. "*Synthesis and characterization of $BaFe_2O_4$ nano-ferrites for gas sensor applications."* Energy, Ecology and Environment **3** (2018): 237-241.

[15] H. Mitsuda, S. Mori and C. Okazaki. "*The crystal structure of barium monoferrite, $BaFe_2O_4$.*" Acta Crystallographica Section B: Structural Crystallography and Crystal Chemistry **27** (1971): 1263-1269.